



相位屏法仿真海洋湍流激光传输特性有效性

牛超君 王晓斌 卢芳 韩香娥

Validity of beam propagation characteristics through oceanic turbulence simulated by phase screen method

Niu Chaojun, Wang Xiaobin, Lu Fang, Han Xiang'e

在线阅读 View online: <https://doi.org/10.3788/IRLA20190452>

您可能感兴趣的其他文章

Articles you may be interested in

非均匀辛格相关蓝绿激光波束通过海洋湍流的传输特性

Propagation characteristics of non-uniformly Sinc-correlated blue-green laser beam through oceanic turbulence

红外与激光工程. 2020, 49(6): 20190370-1-20190370-8 <https://doi.org/10.3788/IRLA20190370>

综合斜程传输和光束扩展影响下的大气湍流相位屏组设计

Design of atmospheric turbulence phase screen set under the influence of combined oblique propagation and beam propagation

红外与激光工程. 2019, 48(4): 404003-0404003(8) <https://doi.org/10.3788/IRLA201948.0404003>

受光束漂移影响的深空上行激光通信链路信道容量

Achievable information rate of deep-space laser uplink communication in presence of beam wander effects

红外与激光工程. 2017, 46(10): 1022001-1022001(8) <https://doi.org/10.3788/IRLA201785.1022001>

旋转相位屏的动态大气湍流数值模拟和验证方法

Numerical simulation and validation method of atmospheric turbulence of phase screen in rotation

红外与激光工程. 2017, 46(12): 1211003-1211003(7) <https://doi.org/10.3788/IRLA201746.1211003>

水下湍流连续相位屏生成的仿真研究

Research on simulation of continuous phase screen generation of underwater turbulence

红外与激光工程. 2017, 46(7): 712001-0712001(6) <https://doi.org/10.3788/IRLA201746.0712001>

弱湍流中紫外光非直视分集接收技术的研究

Research on ultraviolet non-line-of-sight diversity reception technology in weak turbulence

红外与激光工程. 2018, 47(12): 1222002-1222002(6) <https://doi.org/10.3788/IRLA201847.1222002>

Validity of beam propagation characteristics through oceanic turbulence simulated by phase screen method

Niu Chaojun, Wang Xiaobin, Lu Fang, Han Xiang'e*

(School of Physics and Optoelectronic Engineering, Xidian University, Xi'an 710071, China)

Abstract: Oceanic turbulence is an important factor to restrict the application of underwater optical communication. Phase screen method is a simple and effective way to simulate the propagation process of complex beams through turbulence. The constraints of parameter setting for phase screen simulated oceanic turbulence based on the sampling principle and turbulence effects were firstly discussed here. Furthermore, the theoretical expressions of propagation characteristics of Gaussian beam through oceanic turbulence from weak to strong fluctuation regime were derived. Our goal in this research was to testify the validity of phase screen method in oceanic turbulence by comparison of major statistical characteristics of Gaussian beam propagating in oceanic turbulence simulated by phase screen method and the theoretical expressions derived. Results show good match between simulation results and theory formulas for long exposure beam radius and centroid displacement under different turbulence conditions, as well as the scintillation index under weak fluctuation regime. However, results show significant mismatch between numerically estimated and theoretically predicted values for the on-axis scintillation index in strong fluctuation regime.

Key words: oceanic turbulence; phase screen method; beam wander; scintillation index

CLC number: TN249 **Document code:** A **DOI:** 10.3788/IRLA20190452

相位屏法仿真海洋湍流激光传输特性有效性

牛超君, 王晓斌, 卢芳, 韩香娥*

(西安电子科技大学物理与光电工程学院, 陕西西安 710071)

摘要: 海洋湍流是制约水下激光通信应用的重要因素之一, 相对于大气湍流, 海洋湍流在较短距离内即可达到强起伏, 针对强湍流传输特性及数值仿真的可靠性验证具有重要意义。基于大气湍流传输特性理论公式, 利用大气湍流参数等效表达海洋湍流的方法给出了弱起伏到强起伏条件下海洋湍流传输特性的理论计算公式。针对相位屏法在海洋湍流仿真中的应用, 给出了选取相位屏间距、网格尺寸和网格数目的基本要求, 并数值仿真了海洋湍流不同参数条件下的传输特性, 与理论计算结果进行了对比。结果表明: 基于相位屏法得到的光强一阶矩传输特性参量与解析结果较为一致, 但是在强闪烁条件下数值仿真光强闪烁特性与理论结果偏差较大。

关键词: 海洋湍流; 相位屏方法; 光束漂移; 闪烁指数

收稿日期: 2019-12-05; 修订日期: 2020-03-20

基金项目: 高等学校学科创新引智计划 (B17035)

作者简介: 牛超君 (1991-), 女, 博士生, 主要从事大气传输特性及自适应光学方面的研究。Email: niuchaojun123@163.com

导师简介: 韩香娥 (1962-), 女, 教授, 博士生导师, 博士, 主要从事光传输、激光雷达和散射方面的研究。Email: xd_xehan@163.com

0 Introduction

In recent years, underwater laser communication system has attracted more and more attentions. Oceanic turbulence is one of the main concerns for research of laser beams propagating through the ocean^[1-2]. Phase screen method is a simple and effective way to simulate the propagation process of complex beams through random medium^[3-4]. On one hand, the randomness of each realization could provide good reference for experiments. On the other hand, the statistical property of multiple realizations also testify the theory formulas. Recently, phase screen method has been used to simulate oceanic turbulence^[5-6]. Since oceanic turbulence has more influence factors and usually much stronger than atmospheric turbulence, it is necessary to discuss the principle of parameter settings for oceanic turbulence simulated by phase screen method and compare the results calculated by theoretical formula and numerical simulation to confirm the accuracy.

In this paper, the equation of beam spreading, beam wander and scintillation of Gaussian beam propagating through oceanic turbulence are derived follow the theory of beam propagation through random media^[7]. According to the phase screen method used for atmospheric turbulence simulation, the rule of parameter setting for phase screen method used for oceanic turbulence simulation are given. At last, the theoretical computation results and simulation results for statistical property of Gaussian beam propagating through oceanic turbulence are compared and results testify the validity range of phase screen simulated oceanic turbulence.

1 Theory of propagation characteristics

The spatial power spectrum of the refractive-index fluctuations for the oceanic turbulence can be described as^[8]

$$\Phi_n(\kappa) = 0.388 \times 10^{-8} \varepsilon^{-1/3} \kappa^{-11/3} [1 + 2.35(\kappa\eta)^{2/3}] \times \frac{\chi_T}{\omega^2} [\omega^2 \exp(-A_T \delta_{TS}) + \exp(-A_S \delta_{TS}) - 2\omega \exp(-A_{TS} \delta_{TS})] \quad (1)$$

Here, ε is the rate of dissipation of kinetic energy per unit mass of fluid ranging from $10^{-1} - 10^{-10} \text{ m}^2 \text{ s}^{-3}$; χ_T is

the rate of dissipation of mean-squared temperature with the range $10^{-4} - 10^{-10} \text{ K}^2 \text{ s}^{-1}$; ω is the ratio of temperature and salinity contributions to the refractive index spectrum varying in $-5-0$ corresponding to dominating temperature-induced and salinity-induced turbulence, respectively; η is the Kolmogorov micro scale. $A_{TS} = 9.41 \times 10^{-3}$, $A_S = 1.9 \times 10^{-4}$, $A_T = 1.863 \times 10^{-2}$, $\delta_{TS} = 8.284(\kappa\eta)^{4/3} + 12.987(\kappa\eta)^2$.

Ref.[5] introduces the basic expressions of Gaussian beam propagate through random media. The long-term spot radius W_{LE} through turbulence is defined as

$$W_{LE} = W \sqrt{1+T} \quad (2)$$

$$T = 4\pi^2 k^2 L \int_0^1 d\xi \int_0^\infty d\kappa \kappa \Phi_n(\kappa) \times \left[1 - \exp\left(-\frac{\Lambda L \kappa^2 \xi^2}{k}\right) \right] \quad (3)$$

Here, $W = w_0 / \sqrt{\Theta^2 + \Lambda^2}$, w_0 is the initial spot size. Based on the general model, beam wander through turbulence can be expressed as

$$\langle r_c^2 \rangle = 4\pi^2 k^2 L \int_0^1 d\xi \int_0^\infty d\kappa \kappa \Phi_n(\kappa) H_{LS} \left[1 - \exp\left(-\frac{\Lambda L \kappa^2 \xi^2}{k}\right) \right] \quad (4)$$

Large-scale filter function H_{LS} is

$$H_{LS} = \exp\left\{-\kappa^2 W_0^2 \left[(\Theta_0 + \Theta_0 \xi)^2 + \Lambda_0^2 (1 - \xi)^2 \right]\right\} \quad (5)$$

The on-axis scintillation of Gaussian beam through turbulence is

$$\sigma_I^2(0, L) = 8\pi^2 k^2 L \int_0^1 d\xi \int_0^\infty d\kappa \kappa \Phi_n(\kappa) \exp\left(-\frac{\Lambda L \kappa^2 \xi^2}{k}\right) \times \left\{ 1 - \cos\left[\frac{L \kappa^2}{k} \xi (1 - (1 - \Theta) \xi)\right] \right\} \quad (6)$$

Following the approach derived in Ref.[7], A_0 and Θ_0 are defined to characterize the unperturbed beams in terms of the initial phase front radii of curvature F_0 and spot size w_0 :

$$A_0 = \frac{2L}{k w_0^2}, \Theta_0 = 1 - \frac{L}{F_0} \quad (7)$$

Collimated Gaussian beam with $F_0 = \infty$ is considered in this paper. Also, k represents the wavenumber, and L is the propagation path length. Λ and

Θ can also be used to simplify the mathematical expressions

$$\Lambda = \frac{\Lambda_0}{\Theta_0^2 + \Lambda_0^2}, \Theta = \frac{\Theta_0}{\Theta_0^2 + \Lambda_0^2} \quad (8)$$

Since oceanic turbulence could achieve strong fluctuation in a short distance, the theory formula should apply to from weak to strong fluctuation conditions. The method of effective beam parameters maybe used to extend these following formulas into the strong regime by replacing Λ and Θ by their effective beam parameters

$$\Lambda_e = \frac{\Lambda}{1 + 4q\Lambda/3}, \Theta_e = \frac{\Theta - 2q\Lambda/3}{1 + 4q\Lambda/3} \quad (9)$$

Substituting Eq.(1) into Eq.(2)–(6), the long-exposure beam radius W_{LE} , beam centroid displacement σ_c and on-axis scintillation index σ_I^2 for Gaussian beam propagating through oceanic turbulence can be derived.

2 Phase screen method for oceanic turbulence

2.1 Introduction of phase screen method

The principle of phase screen method [7] is considering the beam propagate through vacuum and phase screens along the transmission path alternately as shown in Fig.1. The propagation distance L is divided into many parts, turbulence effects of each part is considered to be a phase screen, the light field between two adjacent phase screen can be expressed as

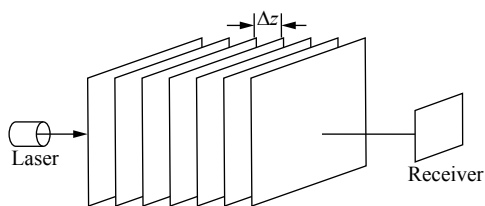


Fig.1 Diagram of phase screen simulation method

$$u(r, z_{j+1}) = F^{-1}\{F[u(r, z_j) \exp[i\varphi(x, y)]] \times \exp(-i \frac{\kappa_x^2 + \kappa_y^2}{2k} \Delta z_{j+1})\} \quad (10)$$

Here, $\Delta z_{j+1} = z_{j+1} - z_j$ is the distance between two phase screen located at z_{j+1} and z_j ; κ_x and κ_y denotes the spatial frequency, the grids are divided to be $N \times N$ and

the resolution is Δx , F and F^{-1} represents Fourier transform and Fourier inverse transform, respectively; $\varphi(x, y)$ reveals the phase fluctuation caused by turbulence which can be expressed as [7]

$$\varphi(x, y) = C \sum_{\kappa_x} \sum_{\kappa_y} a(\kappa_x, \kappa_y) \sqrt{\Phi_\theta(\kappa_x, \kappa_y)} \times \exp[i(\kappa_x x + \kappa_y y)] \quad (11)$$

Here, $x = m\Delta x$, $y = n\Delta y$ represents the spatial domain, Δx , Δy is the sample interval, m, n are integers; $\kappa_x = m' \Delta \kappa_x$, $\kappa_y = n' \Delta \kappa_y$ represents the frequency domain, $\Delta \kappa_x, \Delta \kappa_y$ is the sample interval, m', n' are integers; $a(\kappa_x, \kappa_y)$ is the Fourier transform of the Gaussian random matrix with the mean value 0 and variance 1; $\Phi_\theta(\kappa_x, \kappa_y)$ represents the phase power spectrum, which is related to the power spectrum as

$$\Phi_\theta(\kappa_x, \kappa_y) = 2\pi k^2 \int_z^{\Delta z} \Phi_n(\kappa_x, \kappa_y, \xi) d\xi \quad (12)$$

2.2 Principle of parameter setting

The parameter of phase screen mainly include the grid size Δx , screen size x and the number of phase screen along the propagation path N_{PS} . Since FFT method is usually used to calculate the beam propagation for program, the sample rule request is derived by Ref.[9]

$$\Delta x = \frac{\lambda L}{x} \quad (13)$$

Here, λ is wavelength; L is the propagation distance. Considering that $x = \sqrt{\lambda L N}$, $\Delta x = \sqrt{\lambda L / N}$, the relationships between grid size Δx , screen size x and grids number N is decided. Usually the grids number N is decided firstly, and with higher N , the resolution of sample is more approximate while the computation complexity is higher. In this paper, the influence of different N is shown and compared.

Meanwhile, the description of beam should also be considered. For Gaussian beam, the beam width w_0 should be much bigger than Δx . Also, consider about the characteristics of turbulence, the sampling should be less than half of the coherence length $\Delta x \leq r_0/2$. Here the oceanic turbulence coherence length $r_0 \approx 2.1\rho_0$ [10], spatial

coherence scale ρ_0 for oceanic turbulence is derived by Ref.[11].

$$\begin{aligned} \rho_0 &= [3.603 \times 10^{-7} k^2 \Delta z \varepsilon^{-1/3} \frac{\chi_T}{2\omega^2} (16.958\omega^2 - 44.175\omega + 118.923)]^{-1/2} \quad (\rho_0 \ll \eta) \\ \rho_0 &= [3.603 \times 10^{-7} k^2 \Delta z \varepsilon^{-1/3} \frac{\chi_T}{2\omega^2} (1.116\omega^2 - 2.235\omega + 1.119)]^{-3/5} \quad (\rho_0 \gg \eta) \end{aligned} \quad (14)$$

The number of phase screen along the path is decided by the turbulence strength. According to Ref.[12], the fluctuation between two phase screens should be small enough and meet the requirements of Rytov variance $\sigma_R^2(\Delta z) < 0.1$, then the requirement of phase screen number could be expressed as

$$N_{PS} > [10\sigma_R^2(L)]^{6/11} \quad (15)$$

Rytov variance σ_R^2 can be approximately expressed as^[13]:

$$\sigma_R^2 = 3.063 \times 10^{-7} k^{7/6} L^{11/6} \varepsilon^{-1/3} \chi_T (0.358\omega^2 - 0.725\omega + 0.367) / \omega^2 \quad (16)$$

The example of parameter settings is as follows:

(1) Consider about the strongest turbulence condition as an example, $L=50$ m, $\varepsilon = 10^{-6} \text{m}^2 \text{s}^{-3}$, $\chi_T = 10^{-6} \text{K}^2 \text{s}^{-1}$, $\omega = -2$. Substituting into Eq.(14), $r_0 \approx 0.7$ mm is obtained. Consider that $\Delta x \leq r_0/2$, $\Delta x \ll w_0$, the grid size should fulfill $\Delta x \leq 0.35$ mm, grids number should fulfill $N \geq 238$.

(2) Use Eq.(15) to calculate the phase screen number, and the distance between adjacent phase screens are should meet $\Delta z \leq 2.5$. During the simulation in this paper, the distance between screens is 2.5 m, which is much lower than the atmospheric turbulence simulation conditions.

2.3 Statistical properties calculation formula

Assuming that the long exposure intensity distribution is Gaussian, the statistical properties calculation could be expressed as^[7]. Long exposure beam footprint radius:

$$W_{LE}^2 = 2 \int_{-\infty}^{\infty} r^2 \langle I(r, L) \rangle dr / \int_{-\infty}^{\infty} \langle I(r, L) \rangle dr \quad (17)$$

Standard deviation of the fluctuation of the instantaneous center of the beam:

$$\sigma_c = \sqrt{\langle r_c^2 \rangle} \quad (18)$$

$$r_c = 2 \int_{-\infty}^{\infty} r I(r, L) dr / \int_{-\infty}^{\infty} \langle I(r, L) \rangle dr \quad (19)$$

On-axis scintillation index:

$$\sigma_I^2 = \langle [I(0, L) - \langle I(0, L) \rangle]^2 \rangle / \langle I(0, L) \rangle^2 \quad (20)$$

Here, $\langle \rangle$ represents the average and r_c is the position of beam center.

3 Comparison of results and analysis

The following values of parameters are used in the calculations unless the statement of other values: wavelength $\lambda = 532$ nm, waist width $w_0 = 10$ mm, inner scale $\eta = 1$ mm, $L = 10$ m, $\varepsilon = 10^{-6} \text{m}^2 \text{s}^{-3}$, $\omega = -2$, $\chi_T = 10^{-6} \text{K}^2 \text{s}^{-1}$. According to the example show in Sect.3.2, the grids of phase screen is $N=1024$ and 2048 , leading to the parameter setting $N = 1024, x = 0.16$ m, $\Delta x = 0.16$ mm and $N = 2048, x = 0.24$ m, $\Delta x = 0.12$ mm, respectively. The distance between screens is 2.5 m. Note that the theory results are calculated by the expressions shown in Sec.2 and the numerical simulation results is obtained by the expressions in Sec.3.3 after the average of 1000 realizations.

The results presented in Fig.2(a) and 2(b) reveal that using phase screen method can achieve good correspondence between theoretical and numerical calculations of such statistical characteristics as long-exposure beam radius W_{LE} and σ_c on the basis of appropriate parameter setting. Higher resolution numerical grid (2048×2048 pixels) leads to better accuracy and longer distance weaken the correspondence. However, Fig.2(c) shows that the scintillation index σ_I^2 , which represents the statistical characteristics of second moment of intensity, only have good agreement between theory and numerical results in short distance propagation and the increasement of grids does not make much change to the results.

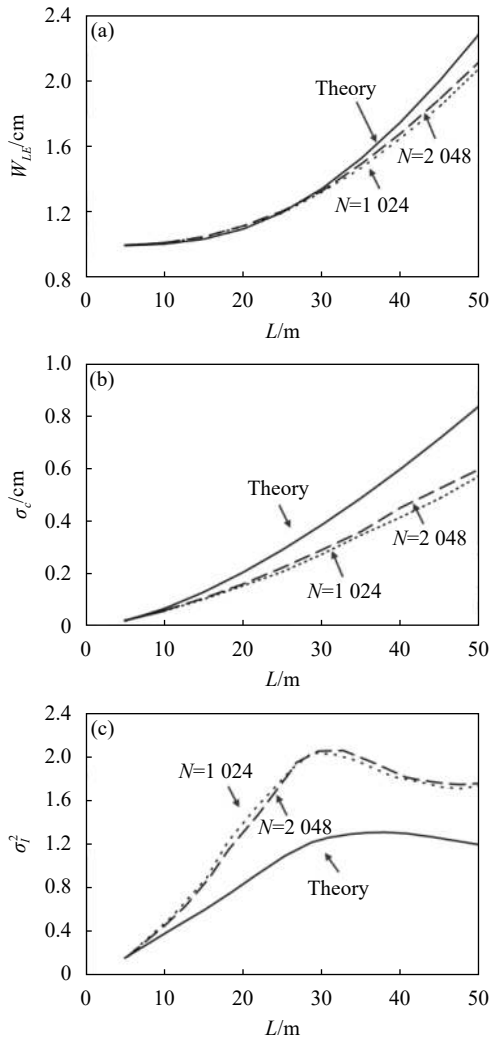


Fig.2 Propagation characteristics versus different propagation distance, (a) long-exposure beam radius W_{LE} , (b) beam centroid displacement σ_c , (c) on-axis scintillation index σ_I^2

Fig. 3–5 shows the similar tendency as Fig.2 that the analytical formula and phase screen numerical simulation for beam spreading and beam wander of Gaussian beam through oceanic turbulence are in good agreements under different turbulence conditions. The simulation results tends to be more approximate when the grids resolution gets higher. Figures also reveal that W_{LE} and σ_c increase when turbulence gets stronger (higher dissipation of mean-squared temperature χ_T , lower rate of dissipation of kinetic energy per unit mass of seawater ε and higher ratio of temperature to salinity contribution ω). However, stronger turbulence affects consistency of the simulation results while the inconsistency keeps under 10%, which

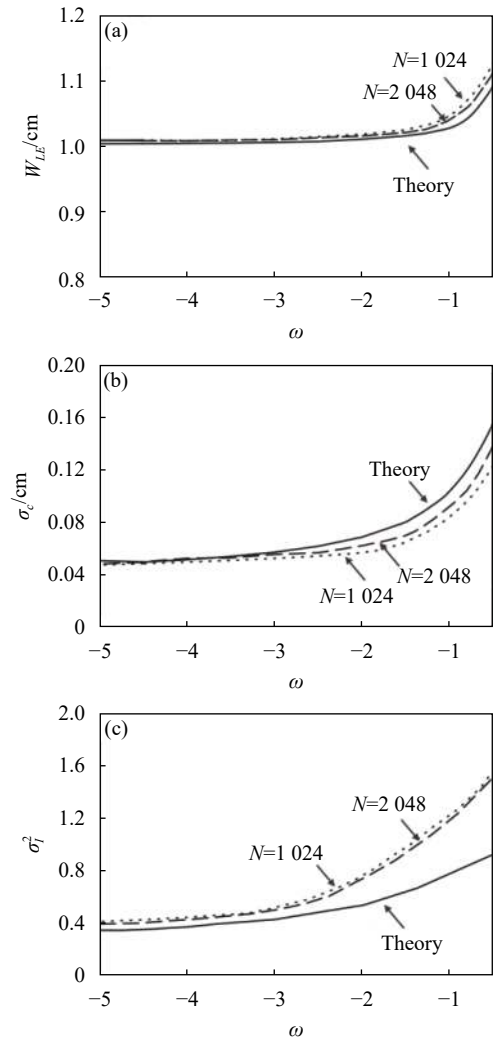


Fig.3 Propagation characteristics versus different ω , (a) long-exposure beam radius W_{LE} , (b) beam centroid displacement σ_c , (c) on-axis scintillation index σ_I^2

illustrates that phase screen method is suitable for being used under different turbulence conditions.

Similar to the results in Fig.2, the on-axis scintillation index σ_I^2 show good match in weak fluctuation regime, the error keeps increase when the turbulence gets stronger $\sigma_I^2 > 1$. The similar significant mismatch between numerical simulations and theoretical results for the scintillation index have been reported in earlier works about atmospheric turbulence. The reason is explained as the impact of either inner scale effect^[14-15] or beam wander induced scintillations^[16]. Ref.[12] proves that the major reason for this mismatch is the irregular appearance of large-amplitude (giant) irradiance spikes

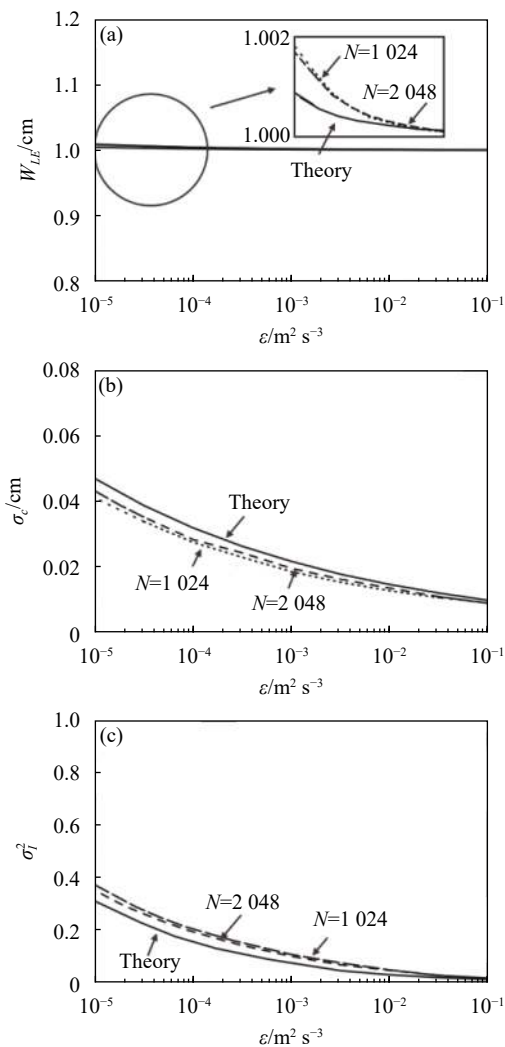


Fig.4 Propagation characteristics versus different ϵ , (a) long-exposure beam radius W_{LE} , (b) beam centroid displacement σ_c , (c) on-axis scintillation index σ_I^2

whose amplitudes greatly exceed the diffraction-limited peaks.

4 Conclusions

In this paper, the analytical formulas of beam spreading, beam wander and scintillation of Gaussian beam through oceanic turbulence are derived. The principle of parameter setting for phase screen simulated oceanic turbulence is mainly discussed and the steps are given in Sec.2.2. Furthermore, the comparison of the simulation results and theory calculation under different parameter settings and different turbulence conditions are shown in figures.

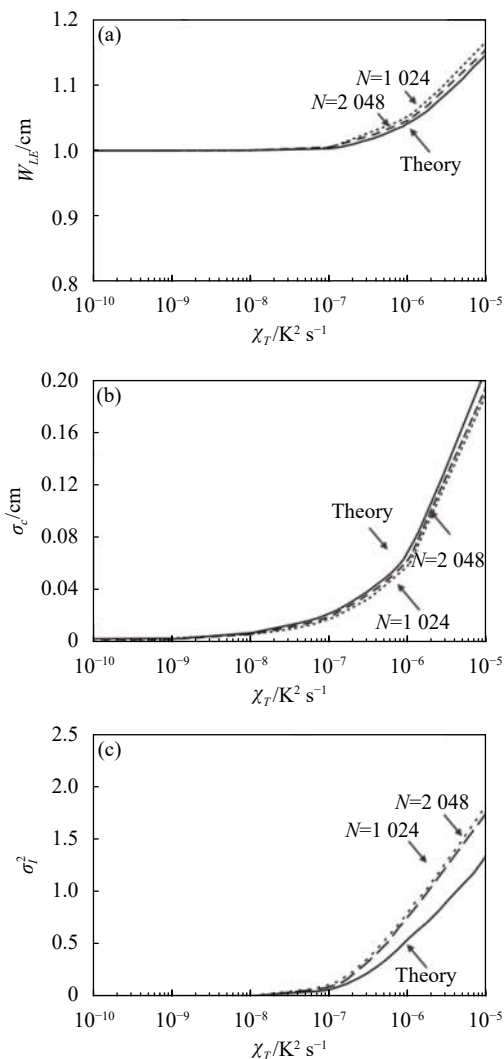


Fig.5 Propagation characteristics versus different χ_T , (a) long-exposure beam radius W_{LE} , (b) beam centroid displacement σ_c , (c) on-axis scintillation index σ_I^2

Results show that beam spreading and beam wander characteristics simulated by phase screen method are in good accordance with the theory formula under different turbulence conditions while the scintillation index has large deviation under strong fluctuation turbulence conditions. In summary, based on appropriate parameter setting, phase screen method can be a simple and effective way to calculate the statistical characteristics depend on the first moment of intensity, such as beam spreading and beam wander. The statistical characteristics depend on the second moment of intensity calculated by numerical simulation achieve good correspondence with theory in

weak fluctuation regime and big mismatch in strong fluctuation regime, which should be further researched in the future.

References:

- [1] Li Y, Yu L, Zhang Y. Influence of anisotropic turbulence on the orbital angular momentum modes of Hermite-Gaussian vortex beam in the ocean [J]. *Optics Express*, 2017, 25(11): 12203.
- [2] Li D, Deng D, Zhao F, et al. Propagation properties of spatiotemporal chirped Airy Gaussian vortex wave packets in a quadratic index medium [J]. *Optics Express*, 2017, 25(12): 13527.
- [3] Xu Chenlu, Hao Shiqi, Zhang Dai, et al. Design of atmospheric turbulence phase screen set under the influence of combined oblique propagation and beam propagation [J]. *Infrared and Laser Engineering*, 2019, 48(4): 0404003. (in Chinese)
- [4] Li Dun, Ning Yu, Wu Wuming, et al. Numerical simulation and verification of dynamic atmospheric turbulence with rotating phase screens [J]. *Infrared and Laser Engineering*, 2017, 46(12): 1211003. (in Chinese)
- [5] Yang T, Zhao S. Study on the Model of Ocean Turbulence Random Phase Screen [J]. *Acta Optica Sinica*, 2017, 37(12): 1201001.
- [6] Niu Chaojun, Lu Fang, Han Xiang'e. Propagation properties of Gaussian array beams transmitted in oceanic turbulence simulated by phase screen method [J]. *Acta Optica Sinica*, 2018, 38(6): 0601004.
- [7] Andrews L, Phillips R. Laser Beam Propagation Through Random Media[M]. Bellingham: SPIE Press, 2005.
- [8] Nikishov V V, Nikishov V I. Spectrum of turbulent fluctuations of the sea-water refraction index [J]. *Fluid Mechanics Research*, 2000, 27(1): 82-98.
- [9] Voelz D, Roggemann M. Digital simulation of scalar optical diffraction: revisiting chirp function sampling criteria and consequences [J]. *Applied Optics*, 2009, 48(32): 6132-6142.
- [10] Fried D. Optical resolution through a randomly inhomogeneous medium for very long and very short exposures [J]. *JOSA A*, 1966, 56(10): 1372-1379.
- [11] Lu L, Ji X, Baykal Y. Wave structure function and spatial coherence radius of plane and spherical waves propagating through oceanic turbulence [J]. *Optics Express*, 2014, 22(22): 27112-27122.
- [12] Lachinova S, Vorontsov M. Giant irradiance spikes in laser beam propagation in volume turbulence: analysis and impact [J]. *Journal of Optics*, 2016, 18(2): 025608.
- [13] Lu Lu. Influence of oceanic turbulence on propagation of laser beams[D]. Hefei: University of Science and Technology of China, 2016: 52-56. (in Chinese)
- [14] Flatte S M, Wang G Y, Martin J. Irradiance variance of optical waves through atmospheric turbulence by numerical simulation and comparison with experiment [J]. *JOSA A*, 1993, 10(10): 2363-2370.
- [15] Consortini A, Cochetti F, Churnside J H, et al. Inner-scale effect on irradiance variance measured for weak-to-strong atmospheric scintillation [J]. *JOSA A*, 1993, 10(11): 2354-2362.
- [16] Andrews L, Phillips R, Ronald L. Strehl ratio and scintillation theory for uplink Gaussian-beam waves: beam wander effects [J]. *Optical Engineering*, 2006, 45(7): 076001.